Int. J. Electrochem. Sci., 14 **(2019)** 9415 – 9427, doi: 10.20964/2019.10.33

International Journal of
ELECTROCHEMICAL
SCIENCE
www.electrochemsci.org

Corrosion Inhibition Effect of Stem Extract of Brahmi (*Bacopa monnieri*) for Mild Steel in Hydrochloric Acid

Chao Wang[1,2], *Peng Liu*[1,2], *Pengcheng Liu* [1,2,*], *Lei Li*[1,2], *Jie Liu*[1,2]

[1] School of Energy Resources, [1] China University of Geosciences, Beijing, 100083, China.
[2] Key laboratory of strategy evaluation for Shale gas, Ministry of Land and Resources, Beijing 100083, China.
[*]E-mail: liupengcheng8883@sohu.com; liupengcheng8883@126.com

Received: 3 June 2019 / *Accepted:* 30 July 2019 / *Published:* 30 August 2019

The stem extract of *Bacopa monnieri* (BMSE) was examined as potential corrosion inhibitor of mild steel in 1 M hydrochloric acid (HCl) media using weight loss, electrochemical and surface studies. The weight loss results discovered that samples covered with BMSE showed less weight loss compared to the samples without BMSE. The electrochemical tests including electrochemical impedance spectroscopy (EIS), and potentiodynamic polarization (PDP) showed good mitigation efficiency of BMSE in 1 M HCl solution. The mixed shift of the anodic and cathodic slopes advised that the inhibitor represented as mixed category. The surface studies were completed using scanning electron microscopy-energy dispersive spectra (SEM-EDS) and atomic force microscopy (AFM). Both the studies displayed even surface in existence of BMSE and rough surface in its absence. All the experimental results are in decent pact respectively.

Keywords: Mild steel, Corrosion inhibition, *Bacopa monnieri*, EIS, AFM, SEM-EDS

1. INTRODUCTION

Mild steel is used all over the world owing its small price and availability. It could be used as a suitable material for oil field storage tanks, transportation pipelines, boilers etc. [1]. The storage tanks store oil for a long period of time. To enhance oil recovery, the tanks are washed with acidizing solutions. Sometimes, to remove the clots or precipitations on the internal side of transportation pipelines they are treated with acidic solutions. These acidizing solutions may cause severe corrosion in the storage tanks, pipelines or oilfield reservoir [2]. This could further lead to accidents, failures and complete shutdown of the place. Internal corrosion is very difficult to measure or to keep a regular watch as the blisters can develop beneath the coating of the pipeline and can grow severely with time. The depth of the pitting or uniform corrosion will increase extensively if not treated well in time. The corrosion will start to form

more pits and cracks throughout the area leading to the failures and accidents. So, there is always a need to develop compounds that can be mixed with acidizing solution to mitigate corrosion during the acidization process.

Although, many corrosion mitigating technique exists, but use of inhibitors is widely used and best practice to effectively mitigate corrosion process. Now, due to strict regulation from the governments and environment regulatory boards the existing compounds cannot be used in higher concentration due to their toxicity level. Adding these substances in lower concentration may not work always depending on the size of the tanks. It is cheap, easily applicable and requires simple instruments. So in order to develop and test ecofriendly compounds, extraction of substances from plants being natural, without toxicity was conducted. Several authors have conduced similar tests and have obtained good results as oilfield inhibitor [3-10]. The achieved results exhibited that plant extracts could function as potential corrosion inhibitors.

Plant extracts are significant as they are ecologically benign and renewable foundation for an extensive variety of desirable mitigators. Natural extracts are regarded as an extremely ironic source of biological mixtures that can be separated by modest techniques with small price. Although, well recognized that inhibition takes place through adsorption of inhibitor molecules on the steel surface. The adsorption can further reflect the nature of inhibition efficiency of the inhibitor depending on chemical, mechanical, physical, and structural properties under given circumstances [11, 12].

The present work explores the impeding outcome of stem extracts of Brahmi *(Bacopa monnieri)* (BMSE) on the mild steel corrosion in 1 M HCl media using the weight loss, electrochemical and surface methods. *Bacopa monnieri* commonly known as Brahmi has its medicinal importance in a number of Ayurvedic medicines. The stem extract is rich in alkaloids, terpenoids and saponins forming the total chemical composition. Due to these chemicals in the extract better mitigating effect is seen for mild steel corrosion in 1 M HCl media. Since, we are focusing on the extract so no methods were employed to separate the components or to study them separately.

2. EXPERIMENTAL SECTION

Mild steel samples of specified dimensions were used for all the tests. The mild steel samples were prepared as test electrodes embedded in epoxy resin with open 1 cm^2 area for electrochemical experiments. The visible surface was rubbed with SiC abrasive paper (different grades), washed carefully and dried prior to use. The acidic solution of 1 M HCl was organized from analytical rated HCl and distilled water. BMSE was prepared using 100 grams of dried powder in 500 ml of purified water after refluxing for 5 hours. The obtained liquid was cleaned several times to eliminate contaminations.

Weight loss experiments were conducted in blank solution and in inhibited solution. The mild steel coupons were weighed and then immersed in the corrosive solution. The coupons were kept in the solution for 3 hours. After the completion of test the coupons were washed with sodium bicarbonate solution and acetone to remove corrosion products and contaminants from the metal surface. The coupons were then dried and weighed again to get the weight loss parameters.

Gamry electrochemical workstation was used to carry out the electrochemical experiments. A traditional three electrode was used together in a cell consisting of a reference electrode, counter electrode and working electrode, respectively. Prior to the start of each experiment, the set up with the complete cell and corrosive solution was allowed to stabilize for 30 minutes. This was conducted to get a stable potential to ensure smooth running of experiments [13]. Electrochemical Impedance Spectroscopy (EIS) experiments were conducted in the 0.0001 Hz to 10 MHz frequency range. The chosen amplitude was 10 mV and the temperature was retained at 308 ± 1 K with the help of a water bath. Echem analyst software that comes with Gamry instrument was used to analyze the obtained results from the tests conducted.

The potentiodynamic polarization tests were carried out from –250 mV to +250 mV at a scan rate of 1 mV s^{-1} [14]. The chosen scan rate is neither too slow nor too fast and it gives the smooth curve without much disturbances. The curves of the anodic and cathodic curves were selected to detect the corrosion current density (i_{corr}), corrosion potential (E_{corr}) and other parameters. For each test, a new metal sample was used and the solution was kept unstirred. All the tests were repeated to ensure the reproducible results.

To test the hydrophillic and hydrophobic behavior of the steel surface, contact angle experiments were done using the drop technique. All the tests were performed using DSA100 Kruss instrument and prior to each test the electrodes were cleaned cautiously to prevent contaminations. The scanning electron microscopy (SEM) and atomic force microscopy (AFM) were done to detect the changes at the surface. SEM-EDS was conducted using SEM-Tescan-Zeiss machine and AFM was done using NDT solver machine. The samples were washed with sodium bicarbonate solution to remove the corrosion products followed by distilled water prior to surface exposure.

3. RESULTS AND DISCUSSION

3.1. Weight loss experiments

3.1.1 Effect of Inhibitor Concentration

The values of the inhibition efficiency (η_w%) achieved through weight loss measurements for diverse concentrations of BMSE in 1 M HCl are given in Table 2. The corrosion tests were executed on triplicate samples and their mean rate of corrosion was determined. The following equation was used to determine the rate of corrosion (C_R) [15]:

$$C_R\,(\mathrm{mm/y}) = \frac{8.76\mathrm{W}}{\mathrm{atD}} \qquad (1)$$

where W be the weight loss, a be the total area, t be the time of immersion (3 hours) and D be density of mild steel in (gcm^{-3}). The subsequent equation was used to determine the inhibition efficiencies (η_w%):

$$\eta_w\% = \frac{WL_{blank} - WL_{inhibitor}}{WL_{blank}} \times 100 \qquad (2)$$

WL_{blank} and $WL_{inhibitor}$ are the corrosion rates without and with extract, respectively.

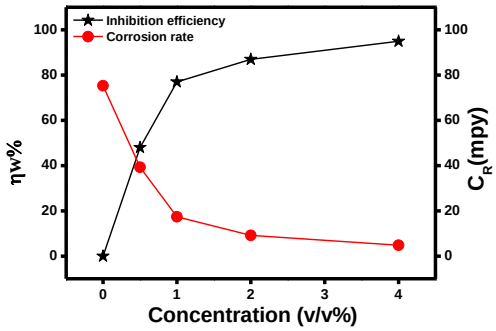

Figure 1. Variation of inhibition efficiency and corrosion rate with change in the concentration of inhibitor.

The efficiency (η_W%) tend to increase with increase in the BMSE concentration and corrosion rate tend to decrease with increase in inhibitor concentration as shown in Figure 1 and Table 1. As inhibition efficiency can be related to the surface coverage, with increase in efficiency surface coverage also increases. Maximum inhibition efficiency is found to be 95% for 4% v/v BMSE. The efficiency did not exceed much after the concentration was increased to 5% and 6%, so 4% is chosen as the optimum concentration for the inhibitor. The adsorption of BMSE on the steel surface took place through the heteroatoms present in the solution that formed a layer on the steel surface and blocked the corrosive media [16, 17].

Table 1. Corrosion parameters for mild steel in 1 M HCl in the absence and presence of BMSE at 308 K for 3 hours.

Inhibitor concentration	Weight loss	C_R	η_W	Surf. Coverage
(v/v%)	(mg cm^{-2})	(mm y^{-1})	(%)	(θ)
Blank	20.3	75.3	-	-
0.5	10.6	39.3	48	0.48
1	04.7	17.4	77	0.77
2	02.5	09.2	87	0.87
4	01.1	04.8	95	0.95

3.1.2. Effect of Temperature

The temperature effect on the corrosion of mild steel in 1 M HCl solution with and without 4% BMSE was conducted using weight loss technique for a duration of 3 hours. The temperature was varied from 308 to 338 K.

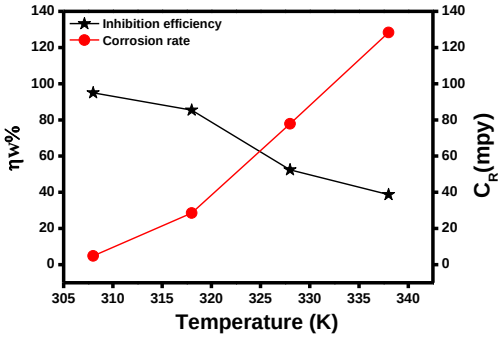

Figure 2. Effect of temperature on corrosion of mild steel in 1 M HCl.

Figure 2 shows the temperature versus inhibition efficiency and corrosion rate diagram. One can keenly observe from the figure that with an increase in temperature the inhibition efficiency decreases and likewise the corrosion rate increases at optimum concentration (4%) of BMSE. This decrease in inhibition efficiency at high temperature suggests that the inhibitor cannot perform at high temperature conditions. The increase in corrosion rate also points towards the aggressiveness of acidic solution at high temperatures. This may be due to desorption of the inhibitor molecules from the mild steel surface that let the corrosive solution to attack the steel surface thereby increasing the rate of corrosion [18]. Also, it may be attributed to the thin film of the inhibitor that was removed or blistered at high temperature. The Arrhenius equation given below was used to determine the activation energy of the process [19]:

$$C_R = \lambda \exp\left(\frac{-E_a}{RT}\right) \quad (3)$$

where C_R represents the rate of corrosion, λ be the constant, E_a represents the activation energy, R be the gas constant, and T be the temperature. The activation energy was determined using the values of log C_R (mpy) and 1/T x 10^{-3} (kelvin).

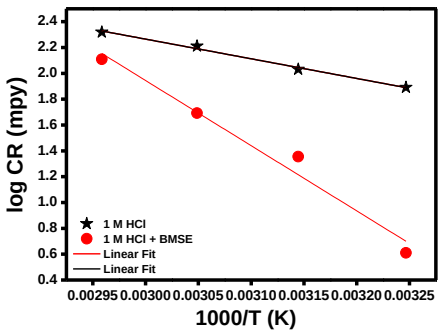

Figure 3. Arrhenius plots of log C_R versus 1/T for mild steel in 1 M HCl with and without BMSE.

The value of activation energy (E_a), 28.5 kJ mg^{-1} for 1 M HCl and 74.2 kJ mg^{-1} of 4% (v/v) BMSE was determined from the slope of the straight line. The greater value of E_a in presence of BMSE is due to the very strong adsorption of BMSE molecules on the steel surface. The molecules formed a

strong film/complex with the metal surface that reduced the active centers and served as a protective layer [20].

3.2 Electrochemical measurements

3.2.1. Electrochemical impedance spectroscopy (EIS) measurements

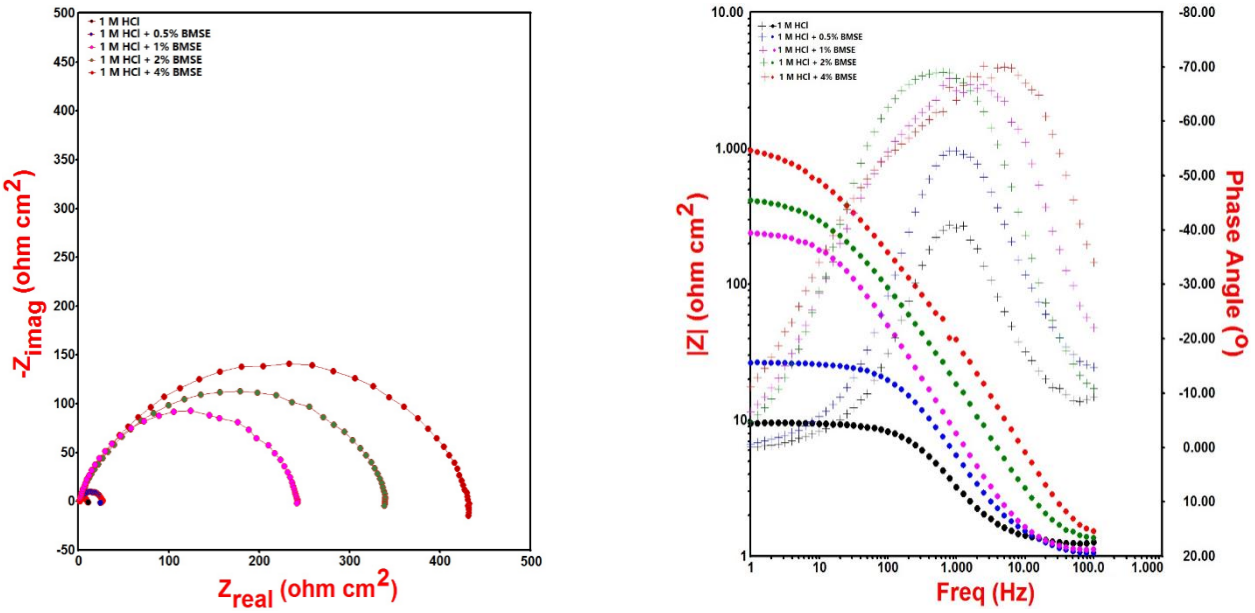

Figure 4. (a) Nyquist and (b) bode-phase angle plots for mild steel in 1 M HCl with and without BMSE.

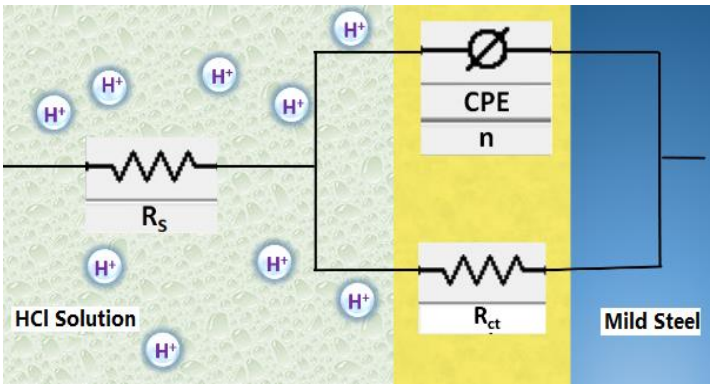

Figure 5. Corresponding Randle's circuit used to fit Nyquist plots in 1 M HCl with various concentrations of BMSE.

Nyquist figures of mild steel in 1 M HCl with and without BMSE are specified in Figure 4a, and it can be detected that the width of the semicircle rises with increasing BMSE adsorption. This rise in semicircles of capacitance recommends that the mitigation behavior of BMSE is due to its adsorption on the mild steel surface without varying the corrosion process [21-25]. Furthermore, Figure 4a shows the higher and lower frequency regions with similar capacitance but with different diameter.

Table 2. Electrochemical impedance parameters for mild steel in 1 M HCl solution with and without BMSE

Inhibitor concentration (v/v%)	R_{ct} (Ω cm^2)	n	Yo ($10^{-6}\Omega^{-1}$ cm^{-2})	C_{dl} (μF cm^{-2})	η%	Slope	Phase angle
Blank	15.2	0.612	219.6	75.7	-	0.455	40.2
0.5	39.7	0.647	192.8	60.1	62	0.488	52.4
1	233.1	0.687	178.4	58.5	93	0.543	63.6
2	319.3	0.734	129.2	42.6	95	0.595	64.9
4	415.5	0.765	94.7	25.5	96	0.649	65.5

In the bode plots (Figure 4b), the slope values tend to increase in existence of BMSE than in its nonexistence (Table 2). This indicates the inhibition action of BMSE on mild steel surface. In phase angle plots (Figure 4b), at the intermediate frequency the height of the peak and phase angle values increases as the BMSE concentration increases. The highest peak at 65.5° (4%) inhibitor concentration for mild steel was observed and reported in Table 2. This is an indication of the development of protective obstacle that causes the isolation of the steel surface from the aggressive solution [26, 27]. Thus, in other words adsorption of the BMSE particles over the steel plays the significant part, which ultimately increased its corrosion resistance property.

The results of the impedance parameters achieved after fitting the experimental data with the corresponding circuit (Figure 5) are tabulated in Table 2. The Randle's equivalent circuit model contains capacitance CPE, which is in parallel with charge transfer resistance (R_{ct}) and they are overall in series with the solution resistance (R_s). The frequency dependent distribution of the current density along the metal surface can be compensated by using the CPE in place of pure capacitor [28, 29]. The CPE impedance (Z_{CPE}) was calculated using the below equation:

$$Z_{CPE} = Y_0[j\omega^{\alpha}]^{-1} \quad (4)$$

where j be an imaginary number ($j = \sqrt{-1}$), Y_o be the admittance and constant for CPE, ω be the angular frequency, and α be the phase change [30]. The addition of BMSE molecules causes the modification of the capacitance parameters owing to the adsorption at the steel-liquid interface. Thus, it become important to calculate the double layer capacitance (C_{dl}) data, because the representation of C_{dl} by CPE and Y_o is not accurate when the values of α is less than 1. The accurate relationship between the C_{dl} and CPE can be calculated using the equation [31]:

$$C_{dl} = Y_o^{1/\alpha}\left[\frac{1}{R_s} + \frac{1}{R_{ct}}\right]^{(\alpha-1)/\alpha} \quad (5)$$

For electrochemical impedance the effectiveness of BMSE was evaluated using the equation below:

$$\eta\% = \frac{R_{ct(i)} - R_{ct(b)}}{R_{ct(i)}} \times 100 \quad (6)$$

where $R_{ct(i)}$ and $R_{ct(b)}$ represent the values of charge transfer resistance with and without BMSE in 1 M HCl correspondingly [32]. According to the Table 2, the R_{ct} values increases and C_{dl} decreases

with the addition of the BMSE to the corrosive solution. This can be ascribed to the adsorption of BMSE fragments over the mild steel surface and reduces the direct contact between the metal and aggressive solution [33]. In addition to this, the increasing values of the efficiency of inhibition in existence of BMSE further support the protection ability of inhibitor.

3.2.2. Polarization measurements

Figure 6 depicts the potentiodynamic polarization pictures of the mild steel with and without BMSE in 1 M HCl media. As can be seen from the figure that both the hydrogen evolution (cathodic) and steel dissolution (anodic) processes were affected after the addition of BMSE in the corrosive solution [34]. Although, the overall mechanism was not affected by the addition of the inhibitor as neither the anodic nor the cathodic shift was observed. The polarization data such as E_{corr}, i_{corr}, and anodic (β_a), and cathodic ($-\beta_c$) slopes were determined from the experiments done using the equation below [35]:

$$\eta_P\% = \frac{i_{corr} - i_{corr(i)}}{i_{corr}} \times 100 \quad (7)$$

i_{corr} and $i_{corr(i)}$ signify the corrosion current density with and without BMSE.

The little shift towards cathodic region after the addition of BMSE, may be owing to the fact that the adsorption of BMSE molecules on the steel surface hindered the corrosive media attack on the working electrode as is evident from the $-\beta_c$ values reported in Table 3 [36]. So, the addition of BMSE in the acidic solution did not changed the overall corrosion mechanism. There was also a little change in the anodic values of β_a that may be attributed to the formation of protective layer of BMSE molecules on the mild steel surface that further blocked the active centers present on the surface, thereby slowing the dissolution process [37, 38].

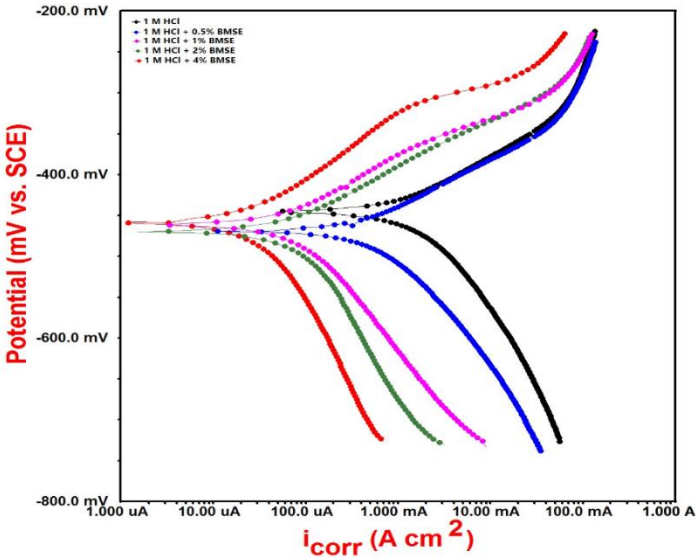

Figure 6. Polarization curves for Al in 1 M HCl in presence of different concentrations of BMSE.

Table 3. Electrochemical polarization parameters for mild steel in 1 M HCl solution with and without BMSE.

Inhibitor	E_{corr}	I_{corr}	β_a	β_c	η_p
(v/v%)	(mV/SCE)	(mA cm^{-2})	(mV dec^{-1})	(mV dec^{-1})	(%)
Blank	–425	259	63	115	–
0.5	–428	189	88	152	27
1	–431	60	70	96	77
2	–437	32	65	93	88
4	–439	14	67	123	95

The maximum inhibition efficiency of 95% at 4% v/v concentration was observed suggesting the lower corrosion rate in presence of inhibitor. The corrosion potential did not showed much variation or shift and was quite stable. The conclusions of research papers suggests that if the shift or displacement in corrosion potential is ≥ 85 mV with respect to the blank (1M HCl) solution, then only an inhibitor can be classified into anodic or cathodic inhibitor [39, 40]. But, from Figure 6 and Table 3, the shift is very evident and is found to be 14 mV. So, based on this theory BMSE can be classified as mixed type inhibitor.

3.3 Surface Characterization

3.3.1. Contact Angle

To detect the surface behavior of mild steel with and without BMSE, contact angle tests were conducted. Contact angle tests can provide essential information regarding the hydrophillic and hydrophobic nature of the steel. The samples were degreased and cleaned several times before test to remove all kinds of contaminants. A baseline establishment was completed after several attempts to perform the tests smoothly using the sessile drop technique. The solution was dropped using a syringe and was repeated for three times to make sure the reproducability of the tests. The 1 M HCl solution without BMSE recorded a lower contact angle of 13.7°. This may be endorsed to the surface of the steel that is in direct contact with the corrosive environment. The corrosive solution can directly attack the steel surface and due to this water loving nature it is termed as hydrophillic surface. Whereas, when the BMSE was added in the solution, it formed a film at the steel surface and due to the presence of this film the contact angle begin to increase. It was 123.5° at 4% v/v concentration suggesting that the film blocked the corrosive solution to reach at the steel surface and this nature is termed as hydrophobic behavior of the surface. So, the surface was hydrophillic without BMSE and hydrophobic with BMSE. This justifies the good inhibiting action of BMSE in 1 M HCl.

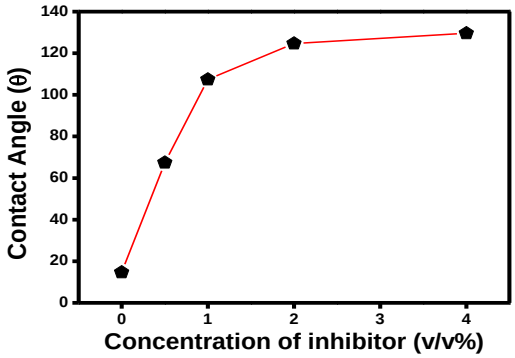

Figure 7. Contact angle for mild steel 1 M HCl in presence and absence of BMSE.

3.3.2 SEM characterization

To observe the extent of protection of the steel surface by BMSE, the morphology of mild steel surface submerged in 1 M HCl without and with 4% BMSE was checked using SEM. In order to get a clear picture of inhibitor action the polished surface was exposed to SEM first and the result is represented in Figure 8a. The polished surface shows the even texture with the lines of abrading. The energy dispersive spectra (EDS) also suggested that the polished surface has mostly iron (Fe) present on the surface. Then the steel surface without BMSE was exposed to the machine and the result is depicted in Figure 8b. The surface with BMSE is very rough, corroded and irregular. The corrosive solution attacked the mild steel surface and due to oxidation the steel formed rust after corroding. Some chloride depositions can also be seen left after the washing process. The surface corroded by 1 M HCl has iron (Fe), gold (Au) (sprayed for better conductivity) and some corrosion products. While, in presence of BMSE the steel surface was smooth, regular and less corroded as shown in Figure 8c. The abraded lines can be seen and the surface is much better than without BMSE. The surface inhibited by the BMSE shows Fe, Cl, and many other atoms that might be present in the inhibitor molecule present on the surface. This proposes that the BMSE formed a shielding layer on the steel surface that inhibited the corrosion process by blocking the corrosive solution from attacking the metal surface.

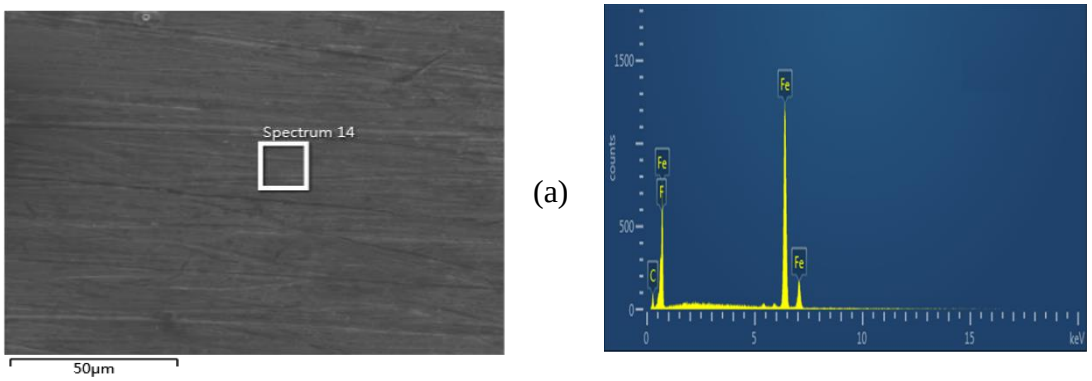

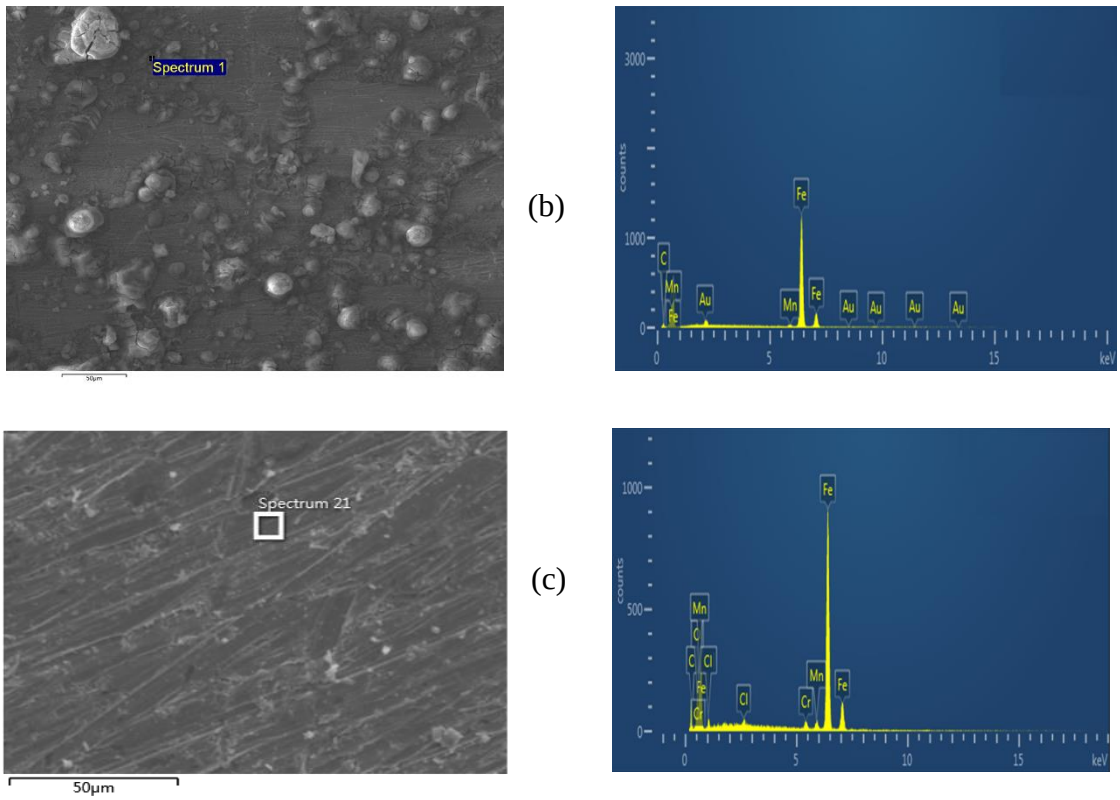

Figure 8. SEM-EDS images for mild steel (a) polished, (b) 1 M HCl, and (c) 4% v/v BMSE.

3.3.3 Atomic Force Microscopy

The 3-D pictures of AFM with and without BMSE inhibitor is shown in Figure 9a, and 9b. As can be understood from Figure 9a the metal surface is strongly damaged without inhibitor and the roughness level is very high. The maximum roughness peak is observed at 262.5 nm for the surface without BMSE. The deep valleys can be seen in the figure shaped due to corrosion on the surface of the steel. On the other hand, BMSE being there, the roughness level is reduced to 65.0 nm and the surface appears to be smooth as shown in Figure 9b [41]. The deep valleys are absent and the surface is much better than without BMSE. So, the mild steel surface is less corroded in existence of BMSE than in its nonexistence.

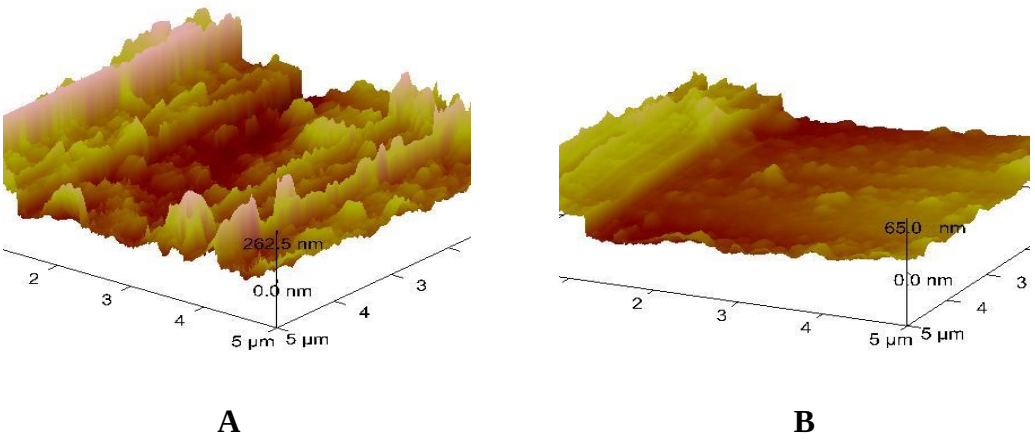

Figure 9. AFM images for mild steel in (a) 1 M HCl, and (b) 4% v/v BMSE.

4. CONCLUSIONS

- Stem extract of *Bacopa monnieri* can be used as potential corrosion inhibitor for mild steel in 1 M HCl solution.
- The weight loss tests showed that the corrosion rate decreases in presence of BMSE while the inhibition efficiency increases.
- The impedance studies revealed that the charge transfer resistance increases in presence of BMSE and double layer capacitance values decreases.
- Polarization studies pointed that the anodic and cathodic shifts are mixed type in nature, so the BMSE could be categorized in mixed class inhibitor.
- Contact angle showed the hydrophobic nature of the steel in presence of BMSE. SEM-EDS and AFM showed the smooth mild steel surface with less roughness in presence of BMSE.

ACKNOWLEDGMENT
The authors would like to thank the Fundamental Research Funds for the Central Universities of China (2652018240), and the Science and Technology Special Funds of China (2016ZX05015-002, 2016ZX05016-006) for financially supporting this research.

References

1. M. Finšgar and J. Jackson, *Corros. Sci*., 86 (2014) 17.
2. R. Wang and S. Luo, *Corros. Sci*., 68 (2013) 119.
3. M. A. Bedair, M. M. B. El-Sabbah, A. S. Fouda and M. Elaryian, *Corros. Sci*., 128 (2017) 45.
4. K.C. Emregul and A. Abbas Aksut, *Corros. Sci.,* 42 (2008) 2051.
5. M.M. Solomon, S.A. Umoren, I.I. Udosoro and A.P. Udoh, *Corros. Sci*., 52 (2010) 1317.
6. L. Zhou, Y. L. Lv, Y. X. Hu, J. H. Zhao, X. Xia and X. Li, *J. Mol. Liq*., 249 (2018) 179.
7. A. A. Olajire, *J. Mol. Liq*., 248 (2017) 775.
8. Ambrish Singh, K. R. Ansari, M. A. Quraishi, Hassane Lgaz and Yuanhua Lin, *J. Alloys Comp*., 762 (2018) 347.
9. A. Singh, I. Ahamad and M. A. Quraishi, *Arab. J. Chem.*, 9 (2016) S1584.
10. A. Yousefi, S. Javadian, N. Dalir, J. Kakemam and J. Akbari, *RSC Adv*., 5 (2015) 11697.
11. K. Azzaoui, E. Mejdoubi, S. Jodeh, A. Lamhamdi, E. Rodriguez-Castellón, M. Algarra, A. Zarrouk, A. Errich, R. Salghi and H. Lgaz, *Corros. Sci*., 129 (2017) 70.
12. M. Mobin, M. Basik and J. Aslam, *Measurement*, 134 (2019) 595.
13. A. A. Khadom, A. N. Abd and N. A. Ahmed, *South Afri. J. Chem. Eng*., 25 (2018) 13.
14. E. B. Ituen, O. Akaranta and S. A. Umoren, *J. Mol. Liq*., 246 (2017) 112.
15. M. M. Askari, S. G. Aliofkhazraei and A. Hajizadeh, *J. Nat. Gas Sci. Eng*., 58 (2018) 92.
16. A. Singh, Y. Lin, W. Liu, D. Kuanhai, J. Pan, B. Huang,C. Ren and D. Zeng, *J. Tai. Inst. Chem. E.*, 45 (2014) 1918.
17. A. Singh, Y. Lin, M. A. Quraishi, O. L. Olasunkanmi, O. E. Fayemi, Y. Sasikumar, B. Ramaganthan, I. Bahadur, I. B. Obot, A. S. Adekunle, M. M. Kabanda and E. E. Ebenso, Molecules, (2015) 122.
18. Ambrish Singh, Y. Lin, W. Liu, S. Yu, J. Pan, C. Ren and D. Kuanhai, *J. Ind. Eng. Chem.*, 20 (2014) 4276.
19. D.D. Macdonald, S. Real and M. Urquidi-Macdonald, *J. Electrochem. Soc.*, 135 (1988) 2397.

20. D. Chu and R.F. Savinel, *Electrochim. Acta*, 36 (1991) 1631.
21. A.M. Abdel-Gaber, E. Khamis, H. Abo-ElDahab and Sh. Adeel, *Mater. Chem. Phys.*, 109 (2008) 297.
22. S.S. Zhang and T.R. Jow, *J. Power Sources*, 109 (2002) 458.
23. A.A. El Hosary, R.M. Saleh and A.M. Shams El Din, *Corros. Sci.*, 12 (1972) 897.
24. M.A. Quraishi, A. Singh, V.K. Singh, D.K. Yadav and A.K. Singh, *Mater. Chem. Phys*., 122 (2010) 114.
25. A. Singh, I. Ahamad, V.K. Singh and M.A. Quraishi, *J. Sol. State Electrochem*., 15 (2011) 1087.
26. G. Gunasekaran and L.R. Chauhan, *Electrochim. Acta*, 49 (2004) 4387.
27. Ambrish Singh, K.R. Ansari, Jiyaul Haque, Parul Dohare, Hassane Lgaz, Rachid Salghi and M.A. Quraishi, *J. Taiwan Inst. Chem. E*., 82 (2018) 233.
28. A.Y. El-Etre, M. Abdallah and Z.E. El-Tantawy, *Corros. Sci.*, 47 (2005) 385.
29. Ambrish Singh, Y. Lin, I. B. Obot, E. E. Ebenso, K. R. Ansari and M. A. Quraishi, *Appl. Surf. Sci*., 356 (2015) 341.
30. E.E. Oguzie, *Corros. Sci.*, 49 (2007) 1527.
31. A. Singh, Y. Lin, E. E. Ebenso, W. Liu and B. Huang, *Int. J. Electrochem. Sci*., 9 (2014) 5993.
32. A. Singh, E. E. Ebenso, M. A. Quraishi and Y. Lin, *Int. J. Electrochem. Sci*., 9 (2014) 7495.
33. A. Singh, I. Ahamad, V. K. Singh and M. A. Quraishi, Chem. *Engg. Com.*, 199 (2012) 63.
34. Z. Tao, S. Zhang, W. Li and B. Hou, *Ind. Eng. Chem. Res.*, 50 (2011) 6082.
35. E.S. Ferreira, C. Giacomelli, F.C. Giacomelli and A. Spinelli, *Mater. Chem. Phys.*, 83 (2004) 129.
36. D.D. Macdonald, *Electrochim. Acta*, 35 (1990) 1509.
37. K.-K. Lee and K.-B. Kim, *Corros. Sci.*, 43 (2001) 561.
38. A. Singh, K.R. Ansari, A. Kumar, W. Liu, C. Songsong and Y. Lin, *J. Alloys Comp.*, 712 (2017) 121.
39. A. Singh, Y. Lin, E. E. Ebenso, W. Liu, J. Pan and B. Huang, *J. Ind. Eng. Chem*., 24 (2015) 219.
40. E. Khamis, *Corrosion*, 46 (1990) 476.
41. A. Singh, Yuanhua Lin, K. R. Ansari, M. A. Quraishi, E. E. Ebenso, Songsong Chen and W. Liu, *Appl. Surf. Sci*., 359 (2015) 331.